Environmental Science
Processes & Impacts

PAPER

View Article Online
View Journal | View Issue

Cite this: *Environ. Sci.: Processes Impacts*, 2016, **18**, 844

Landscape geomorphic characteristic impacts on greenhouse gas fluxes in exposed stream and riparian sediments

Philippe Vidon* and Satish Serchan†

While excessive releases of greenhouse gases (GHG: N_2O, CO_2, CH_4) to the atmosphere due to the burning of fossil fuel remains a concern, we also need to better quantify GHG emissions from natural systems. This study investigates GHG fluxes at the soil–atmosphere interface in a series of 7 stream reaches (riparian zones + exposed streambed sediment) across a range of geomorphic locations from headwaters reaches to lowland wetland reaches. When riparian fluxes (RZ) are compared to fluxes from in-stream locations (IS) under summer baseflow conditions, total CO_2-equivalent (CO_{2eq}) emissions are approximately 5 times higher at RZ locations than at IS locations, with most CO_{2eq} driven by CH_4 production at RZ locations where wet conditions dominate (headwater wetlands, lowland wetlands). On a gas-by-gas basis, no clear differences in N_2O fluxes between RZ and IS locations were observed regardless of locations (headwater *vs.* lowland reaches), while CO_2 fluxes were significantly larger at RZ locations than IS locations. Methane fluxes were significantly higher in wetland-influenced reaches than other reaches for both RZ and IS locations. However, GHG fluxes were not consistently correlated to DOC, DO, NO_3^-, NH_4^+, or water temperature, stressing the limitations of using water quality parameters to predict GHG emissions at the floodplain scale, at least during summer baseflow conditions. As strategies are developed to further constrain GHG emission for whole watersheds, we propose that approaches linking landscape geomorphic characteristics to GHG fluxes at the soil–atmosphere interface offer a promising avenue to successfully predict GHG emissions in floodplains at the watershed scale.

Received 15th March 2016
Accepted 9th June 2016

DOI: 10.1039/c6em00162a

rsc.li/process-impacts

Environmental impact

This study investigates GHG fluxes at the soil–atmosphere interface in a series of 7 stream reaches (riparian zones + exposed streambed sediment) across a range of geomorphic locations from headwaters reaches to lowland wetland reaches. Total CO_2-equivalent (CO_{2eq}) emissions were approximately 5 times higher at RZ locations than at IS locations, with most CO_{2eq} driven by CH_4 production at RZ locations. However, GHG fluxes were not consistently correlated to DOC, DO, NO_3^-, NH_4^+, or water temperature. As strategies are developed to further constrain GHG emission for whole watersheds, we propose that approaches linking landscape geomorphic characteristics to GHG fluxes at the soil–atmosphere interface offer a promising avenue to successfully predict GHG emissions in floodplains at the watershed scale.

Introduction

While excessive releases of greenhouse gases (GHG: N_2O, CO_2, CH_4) to the atmosphere due to the burning of fossil fuel remains a concern, we also need to better quantify GHG emissions from natural systems.[1] Within this context, many studies have therefore documented GHG fluxes at the soil–atmosphere interface in agricultural lands,[2] forested hillslopes,[3] wetlands[4,5] and, to some extend, riparian zones.[6–8] However, few studies document GHG emissions in exposed streambed sediments at baseflow and in sections of riparian zones immediately near the stream. These areas of the landscape nevertheless generally often present higher amounts of organic matter than hillslopes, higher water availability, and often display unique reducing biogeochemical conditions, which makes these areas of the landscape potential hot spot of GHG emission at the soil–atmosphere interface.[7–10] Recent studies have indeed shown that riparian zones are often hotspot of biogeochemical transformations in the landscape, and that GHG losses from streams

Department of Forest and Natural Resources Management, The State University of New York College of Environmental Science and Forestry (SUNY-ESF), 1 Forestry Drive, Bray 320, Syracuse, NY 13210, USA. E-mail: pgvidon@esf.edu; Fax: +1 315 470 6535; Tel: +1 315 470 4765

† Now at: PhD Student, Water Resources Graduate Program, The Oregon State University (OSU), Corvallis, OR, 97330, USA and Pathways Student, United State Department of Agriculture, Pacific Northwest Research Station, Corvallis Forestry Sciences Laboratory, 3200 SW Jefferson Way, Corvallis, OR 97331, USA, Email: serchans@oregonstate.edu

can be large enough to affect C and N budgets at the continental scale.[9–13]

From a process standpoint, GHG production in soils and sediments (*i.e.*, N_2O, CO_2, CH_4) is predominantly the byproduct of heterotrophic processes.[10,14,15] Under aerobic conditions, O_2 is used as an electron acceptor to oxidize organic matter (electron donor), which leads to the production of CO_2. As conditions become more reduced and O_2 progressively disappears, NO_3^- is used as an electron acceptor to oxidize organic matter (denitrification). Although N_2 gas is generally produced *via* denitrification, N_2O is also released due to incomplete denitrification in most systems. Nitrification (under aerobic conditions) can also generate N_2O, albeit generally at a lower rate than denitrification (under anaerobic conditions). Under strongly reducing conditions, CO_2 can be used as an electron acceptor to oxidize organic matter during methanogenesis, resulting in CH_4 production and CO_2 consumption.[10,14,15] The rate of these reactions in natural systems is predominantly regulated by temperature, organic carbon availability (electron donor), soil moisture/water availability, and electron acceptor dynamics (O_2, NO_3^-, SO_4^{2-}, CO_2).[10,14,15] However, predicting the rate of these reactions and ultimately developing solid estimates of GHG production in natural systems remains a challenge as riparian zones and stream sediments in particular are extremely heterogenous systems.[9,16] For instance, some studies have shown the existence of anoxic patches (denitrification hot spots) in soil aggregates in globally oxic environment in riparian soils,[17] while others have shown strong vertical and horizontal biogeochemical gradients in riparian zones.[18,19] In streams, sediments in pools can be hot spots of CH_4 production due to anoxic conditions associated with lower stream flow velocity and organic matter accumulation, while sediments in riffles are often well oxygenated and may be hot spot of nitrification and denitrification rather than methanogenesis.[11,20,21]

In order to generalize estimates of GHG production at the soil–atmosphere interface in riparian zones and exposed streambed sediments at the watershed scale, it is therefore critical to identify field scale indicators of GHG emission (*e.g.* wetland influenced reaches, headwater *vs.* lowland riparian areas) in addition to well known, yet poorly scalable, biogeochemical indicators such as organic carbon availability, dissolved oxygen, or nitrate/ammonium availability. Within this context, landscape geomorphic characteristics (topography, headwater *vs.* lowland position, surficial geology) have been shown to influence soil biogeochemistry (*i.e.* O_2 supply through soil moisture, substrate availability such as nitrate and organic carbon) and GHG fluxes at the soil–atmosphere interface.[15,22–24] For instance, Riveros-Iregui and McGlynn (2007) showed that landscape positions (*e.g.* riparian zone *vs.* hillslope) impacted CO_2 emission in a Montana forested watershed.[23] Elsewhere, other studies indicate that upland soil environments are often CH_4 sinks,[22] that wetlands are large CH_4 sources,[4] and that riparian areas can significantly contribute to N_2O fluxes.[6,8]

In this study, we therefore investigate GHG fluxes at the soil–atmosphere interface in a series of 7 stream reaches (riparian zones + exposed streambed sediment at baseflow) along a 3.2 km stream with a range of geomorphic conditions from headwaters reaches to lowland wetland reaches. We aim to determine the relative importance of riparian zones *vs.* exposed stream sediments at regulating GHG emissions for each reach, and to understand the roles of topographic location and floodplain geomorphology in influencing GHG fluxes. Within this context, we also discuss the dominant biogeochemical processes driving GHG emissions at each location.

Materials and methods

To achieve the objectives above, we measured N_2O, CO_2, and CH_4 fluxes at the soil–atmosphere interface at 35 riparian locations (RZ) and 35 in-stream (IS) exposed streambed locations on four dates (07/16/2013, 07/25/2013, 08/15/2013, 08/29/2013) in July–August 2013 (summer baseflow) using static chambers, along with local biogeochemical conditions in piezometers in a New York mountain stream.

Specifically, the study took place in Archer Creek, which is located in Archer Creek Watershed (515 m above sea level, 43°59′32″ N, 74°14′32″ W), and is a 135 ha forested catchment (1% water, 6% forested wetland, 93% forest) located in the Adirondack Mountains, NY (Fig. 1). Climate is cool, moist, and continental. Between the years 1941–2007, the mean annual temperature was 5.0 °C, the mean annual precipitation was 1046 mm, and the mean annual snowfall was 303 cm.[25] Precipitation in 2013 was 12% greater than normal and was recorded at the National Atmospheric Deposition Program/National Trends Network Site (ID NY20) located in the Huntington Wildlife Forest approximately 2.0 km from the study stream. The surficial geology of the watershed consists of glacial till composed of approximately 75% sand, and less than 10% clay content.[26] Upland soils are sandy loam (Becket Mundal series) approximately one meter thick with localized areas of deeper soil. Wetlands and valley-bottoms soils are mainly composed of Greenwood Mucky Peats deposits 1 to 5 meters deep.[27] Archer Creek (study stream) is composed of two upper sections (S14 and S15; Fig. 1), both of which begin as seeps.[26,28] Although the average slope for Archer is 11%, S14 and S15 average 16% and 10% slope, respectively.[27]

Two headwater (HW) reaches (HW1 & HW2) were randomly selected in S14, two (HW3 & HW4) were randomly selected in S15, and three (two lowlands: LL1, LL2, and one wetland: WL) were randomly selected in the lower reaches of Archer Creek (AC) (*i.e.* downstream of the S14–S15 confluence). Reaches HW1 and HW3 contain a high amount of mucky wet soils compared to HW2 and HW4 (Fig. 1). Although the LL2 reach was not directly influenced by a wetland like the WL reach, it was wetter (shallower water table) than the rockier LL1 reach higher up in the watershed (Fig. 1). Each reach was 20 m long and 12 m wide, with a 6 m line away from the centerline of the grid marking the outer extend of the study area of each reach for practical purposes (Fig. 1). Within each reach, riparian areas and exposed sediment areas were mapped and 5 riparian locations and 5 exposed in-stream sediment locations were selected to install static chamber (for greenhouse gas measurements) and piezometer clusters (for water quality measurements) (Fig. 1). Piezometers consisted of 50 cm long 1.67 cm ID PVC pipe with

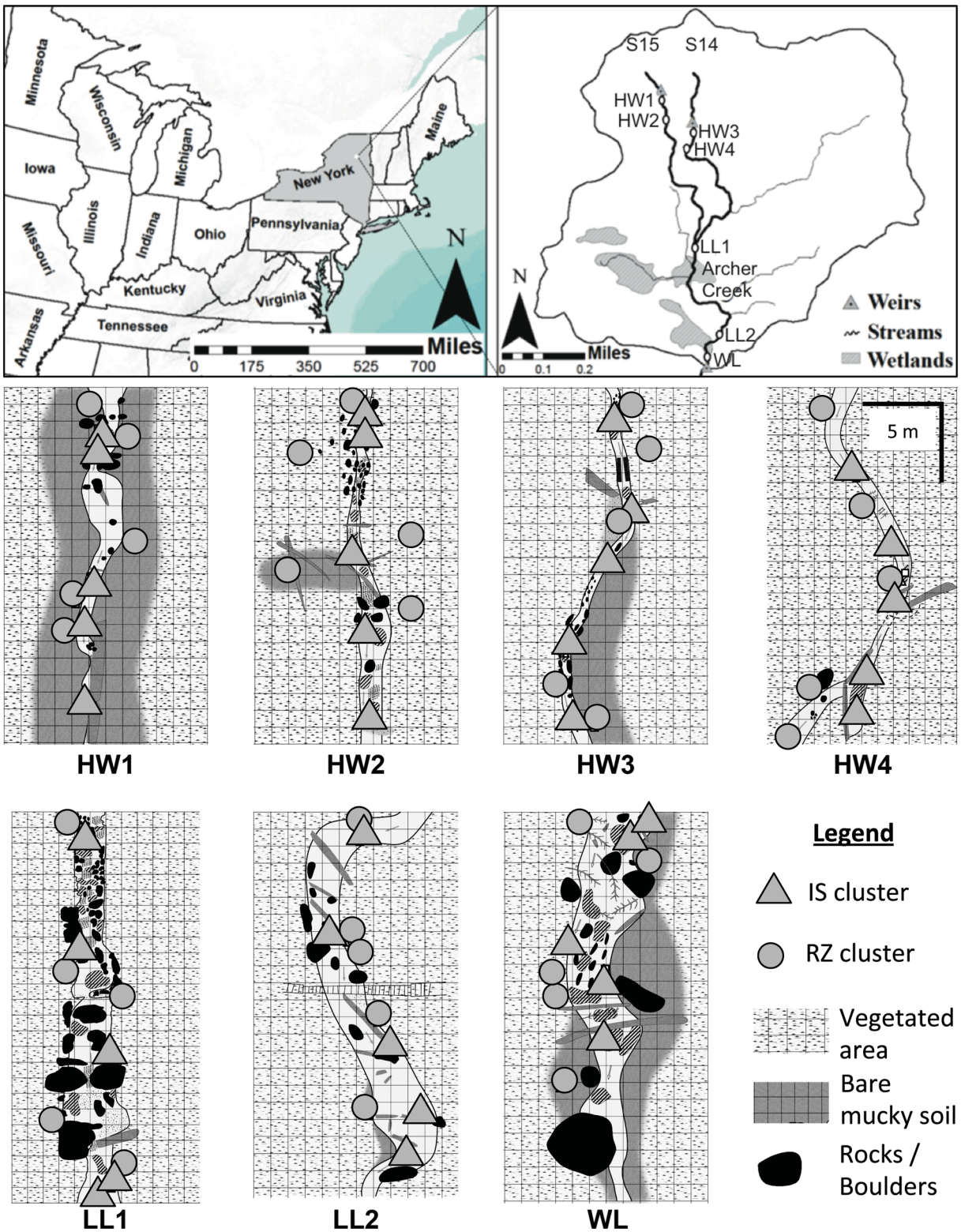

Fig. 1 Archer Creek watershed location in New York, USA (upper left), and locations of the seven stream reaches studied in Archer Creek watershed (upper right). Planar views of the seven stream reaches with in-stream (IS) and riparian (RZ) instrument cluster (piezometers and static chambers) locations (bottom). *Acronyms*: HW1–4 = headwater locations 1 through 4, LL1 and LL2 = lowland locations 1 and 2, WL = wetland location.

20 cm long slotted ends at the bottom, and were installed at a depth of 40 cm below ground surface (BGS) using a screw auger in the riparian zone, and 20–30 cm BGS in exposed stream sediments. On four different dates during the July–August 2013 summer baseflow period, piezometers were purged and approximately 140 mL of water was subsequently collected for analysis. Groundwater temperature and dissolved oxygen (DO) in piezometers were measured in the field using Hanna DO meters (Hanna HI9146, Hanna Instrument Inc. Smithfield, Rhode Island, USA) and Hanna Temp/ORP meters (Hanna HI9125, Hanna Instrument Inc. Smithfield, Rhode Island, USA). Water samples were collected with Tygon tubing using a three-way valve connected to a syringe to prevent contact with the atmosphere while pumping. Dissolved oxygen was then measured with the DO meter by inserting the oxygen probe into the syringe.[19] Water samples were then kept in a cooler and filtered using 0.7 μm GF/F filters (Whatman Inc., Florham Park, New Jersey) that same day. Nitrate (NO_3^-) and ammonium (NH_4^+) were measured on a Bran + Luebbe Autoanalyzer 3 (SEAL Analytical, Mequon, Wisconsin, USA) using standard colorimetric methods.[29] For dissolved organic carbon (DOC) analysis, an aliquot of the samples to be analyzed was acidified using 2 molar H_2SO_4 and refrigerated until analysis for DOC using a Tekmar carbon analyzer (680–1000 °C combustion temperature, Phoenix 8000, Tekmar, Mason, OH). For all water analyses, triplicate analyses were run on 10% of the samples, and check-standards were analyzed for every 10 samples. Detection limits for NO_3^-, NH_4^+, and DOC were 0.01 mg N L^{-1}, 0.005 mg N L^{-1}, and 0.5 mg L^{-1}, respectively.

Gas samples for GHG flux calculations (CH_4, CO_2, and N_2O) at the soil–atmosphere interface were collected using static chambers (35 riparian chambers, 35 exposed stream sediment chambers; Fig. 1) whenever water samples were collected for analysis (4 baseflow dates during the July–August 2013 summer period). Static chambers were made of white PVC material, and consisted of two parts: a bottom section (37 cm height and 27 cm diameter) inserted 10 cm into the ground, and an airtight lid fitted with a gas sampling port.[30] When sampling, the chambers were closed with the lid and headspace gas concentrations measured 3 times over 50 min (0 min, 25 min, 50 min). Air samples (~15 mL) were stored in evacuated vials (10 mL) fitted with gray butyl rubber septa. GHG fluxes (F) were computed as:

$$F = \left(\frac{dC}{dt}\right)\left(\frac{V}{A}\right)k \quad (1)$$

where dC/dt is the linear rate of change in GHG concentration inside the chamber (mass GHG m^3 air per min), V is the chamber volume (m^3), A is the area circumscribed by the chamber (m^2), and k is a unit conversion factor (1440 min per day).[2] Samples were kept out of the light during transport and storage periods, and were usually analyzed within two weeks of collection. Carbon dioxide, CH_4, and N_2O concentrations were analyzed using a Shimadzu GC-2014® gas chromatograph (Shimadzu Corporation, Kyoto, Japan) equipped with a flame ionizing detector (for CO_2 and CH_4) and an electron capture detector (for N_2O) interfaced with a CombiPal® autosampler (LEAP Technologies, Carrboro, North Carolina). The stationary phase consisted of a Porapak Q® precolumn (90 cm long) and Hayesep D® analytical columns (180 cm long). The GC was calibrated using standard gases obtained from Alltech (Deerfield, Illinois). To prevent moisture buildup in the GC columns, the GC oven was heated (150 °C) for 15 min for every 20 samples. In the rare cases when a non-linear relationship was observed ($R^2 < 0.75$) in the chamber, samples were discarded and not included in the analysis. When needed, GHG fluxes were expressed in carbon dioxide equivalent (CO_{2eq}) based on their global warming potential (GWP).[1] For these calculations, CO_2 has a GWP of 1, while N_2O and CH_4 have GWPs of 298 and 25, respectively.[1]

A two-way ANOVA (7 levels of sites (*i.e.* 7 reaches) and 2 levels (*i.e.* riparian *vs.* exposed stream sediments)) was conducted to assess differences between groups. If a significant statistical effect was detected, post hoc pair-wise differences were analyzed using Tukey's multiple comparison tests. To meet the assumption of normality prior to parametric statistical analyses, most data were log transformed and normality determined using an Anderson–Darling test. Linear correlations between each GHG fluxes and predictor variables (DOC, DO, NO_3^-, NH_4^+, Temp) were quantified using Pearson correlation coefficients. Statistical analyses were performed using SAS 9.4/9.3 (SAS Institute Inc., Cary, North Carolina, USA), and boxplots and graphs were generated in Minitab 16 (Minitab Inc., State College, Pennsylvania, USA) and Microsoft Excel 2010 (Microsoft Corporation, Redmond, California, USA).

Results

Water quality measurements: riparian zones (RZ) *vs.* in-stream exposed sediments (IS)

Although dissolved oxygen concentration (DO) varied by location, DO was generally higher at headwater in-stream (IS) exposed sediment locations (HW1, HW2, HW3, HW4) and one of the lowland reaches (LL1) (median DO > 5 mg L^{-1}) than in exposed sediments in the wetland or at most riparian locations (Fig. 2). Within the riparian zone locations (RZ), DO values (range: 2–3 mg L^{-1}) in the WL and LL2 riparian zone were also lower (albeit not significantly) than at other RZ locations (median DO range = 3–6 mg L^{-1}). Opposite of dissolved oxygen, DOC at both IS and RZ locations increased from 1–5 mg L^{-1} at headwater locations, to 6–11 mg L^{-1} at the LL2 and WL locations; however, DOC concentrations generally did not differ significantly between IS and RZ locations (statistics not shown for this comparison). A pattern similar to DOC was observed for NH_4^+, with higher median NH_4^+ concentrations in IS sediment water (0.1–0.2 mg N L^{-1}) and RZ water (0.3–0.5 mg N L^{-1}) at the WL and LL2 locations than at headwater locations HW1–4 (<0.1 mg N L^{-1} in IS sediment water, <0.3 mg N L^{-1} in RZ water). Although NO_3^- concentrations varied significantly throughout the watershed (*e.g.*, >0.4 mg N L^{-1} at the HW4 IS and RZ sites, <0.1 mg N L^{-1} at HW1 sites in RZ water), some of the lowest NO_3^- values were observed at the LL2 and WL sites, and some of the highest at the HW4 sites

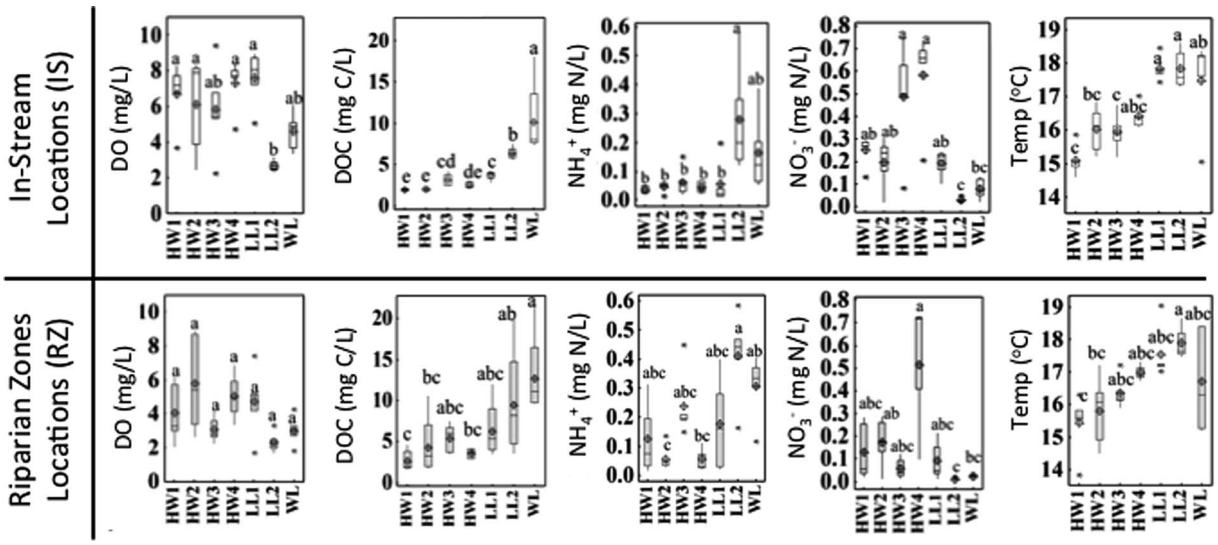

Fig. 2 Box plots (mean, median, 25th and 75th quartiles, and outliers) illustrating dissolved oxygen (DO), dissolved organic carbon (DOC), ammonium (NH_4^+), and nitrate (NO_3^-) concentrations, and groundwater water temperature (°C) in riparian (RZ) and in-stream (IS) piezometers for stream reaches HW1–4, LL1–2, and WL over the study period (see Fig. 1 for acronym definitions).

(both IS and RZ), and HW3 site in exposed stream sediments (IS). Over the course of the 4 sampling dates, groundwater temperatures were similar at RZ and IS sites, and increased from headwater locations (15–17 °C range) to lowland and wetland locations (16–18 °C). At IS locations, the water table (WT) was on average 3.7 cm below ground surface (BGS) across all sites and all sampling dates, with the lowest value (6.9 cm BGS) at the HW4 site, and the highest value (0.6 cm BGS) at the HW3 site. At RZ locations, the water table averaged 6.6 cm BGS over the study period, with the lowest values observed at the HW4 site (15.8 cm BGS) and the highest ones observed at the WL site (2.3 cm BGS).

Greenhouse gas fluxes: riparian zones (RZ) *vs.* in-stream exposed sediments (IS)

On a reach-by-reach basis, median CO_2 fluxes at RZ locations (0.3 g C per m^2 per day at LL1 site to 2.5 g C per m^2 per day at HW3 site) were always higher than at IS locations (0.15 g C per m^2 per day at the HW2 site to 0.72 g C per m^2 per day at the WL site) (Fig. 3). However, although CO_2 fluxes varied by location, no consistent increase or decrease in CO_2 fluxes were observed from headwater sites (HW1–4) to lower elevation sites (LL and WL sites) in either the riparian zone or exposed stream sediments. Unlike for CO_2, N_2O fluxes were not consistently higher at RZ locations than at IS locations. At IS locations, median N_2O

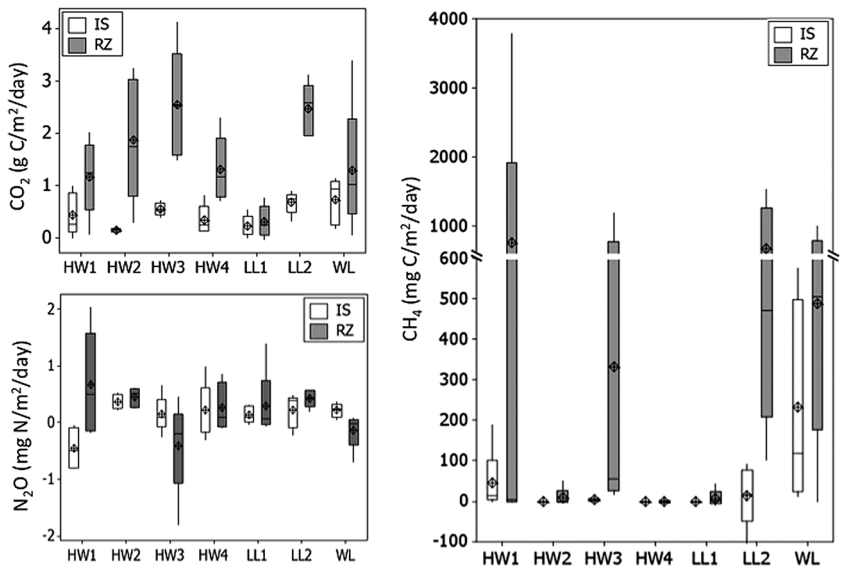

Fig. 3 Box plots (mean, median, 25th and 75th quartiles, and outliers) illustrating CO_2, N_2O and CH_4 fluxes at the soil–atmosphere interface at riparian (RZ) and in-stream (IS) locations for stream reaches HW1–4, LL1–2, and WL over the study period (see Fig. 1 for acronym definitions).

flux values ranged from −0.5 mg N per m^2 per day at the HW1 site to 0.4 mg N per m^2 per day at the HW2 site, while at RZ locations N_2O flux values ranged from −0.14 mg N per m^2 per day at WL site to 0.66 mg N per m^2 per day at HW1 site. Methane fluxes on the other hand exhibited a broad range of variation (as shown by the difference in the median and mean values), especially at RZ locations where mean CH_4 fluxes ranged from −0.13 mg C per m^2 per day at the HW4 site to 766.13 mg C per m^2 per day at the HW1 site, with highest mean (and median) values at the HW1 and HW3 sites (mucky soil-influenced sites) and the lowland (LL2) and wetland sites (WL). At IS locations, mean CH_4 fluxes ranged from −0.05 mg C per m^2 per day at the HW4 site to 232.6 mg C per m^2 per day at the WL site. The HW1 site and LL2 site had the second and third highest mean CH_4 fluxes values at 45.7 mg C per m^2 per day and 15 mg C per m^2 per day, respectively, while negative CH_4 fluxes were observed at the LL1 site (−0.19 mg C per m^2 per day). Within each group (*i.e.* RZ and IS groups), significant differences between locations were primarily observed for CH_4 (Fig. 3).

When converted to CO_{2eq} (see methods) and compared on an area basis (1 m^2), RZ fluxes are up to one order of magnitude higher than CO_{2eq} fluxes at IS locations (Fig. 4), with total CO_2-equivalent (CO_{2eq}) emissions approximately 5 times higher at RZ locations than IS locations. Specifically, at IS locations, total CO_{2eq} fluxes varied from 0.73 g CO_{2eq} per m^2 per day at the HW2 site to 9.27 CO_{2eq} per m^2 per day at the WL site, with most of CO_{2eq} emission stemming from CH_4 fluxes at the WL site, and CO_2 emissions at other locations. At RZ locations, CO_{2eq} fluxes varied from 1.48 CO_{2eq} per m^2 per day at the LL1 site to 28.43 CO_{2eq} per m^2 per day at the LL2 site. At the WL, LL2, HW3, and HW1 sites, CH_4 was the dominant source of CO_{2eq}, while at the other sites, most CO_{2eq} emissions were derived from CO_2 emissions.

When all locations are considered (35 riparian zone locations, 35 stream locations, 4 sampling dates), GHG fluxes either in the riparian zone or in-stream locations were generally not significantly ($r < 0.18$, $n = 140$, $p > 0.05$) correlated to either NO_3^-, NH_4^+, DOC, DO or groundwater temperature, except for CH_4 and DOC across all IS locations and CO_2 and NH_4^+ across all RZ locations (Fig. 5). On site-by-site basis significant correlation exists ($r > 0.43$, $n = 20$, $p < 0.05$) (*e.g.* NO_3^- and N_2O in the riparian zone at LL1, NH_4^+ and CH_4 in the riparian zone at HW2, DO and N_2O at HW3 in IS exposed sediments), but these correlations do not consistently occur across sites (Fig. 5).

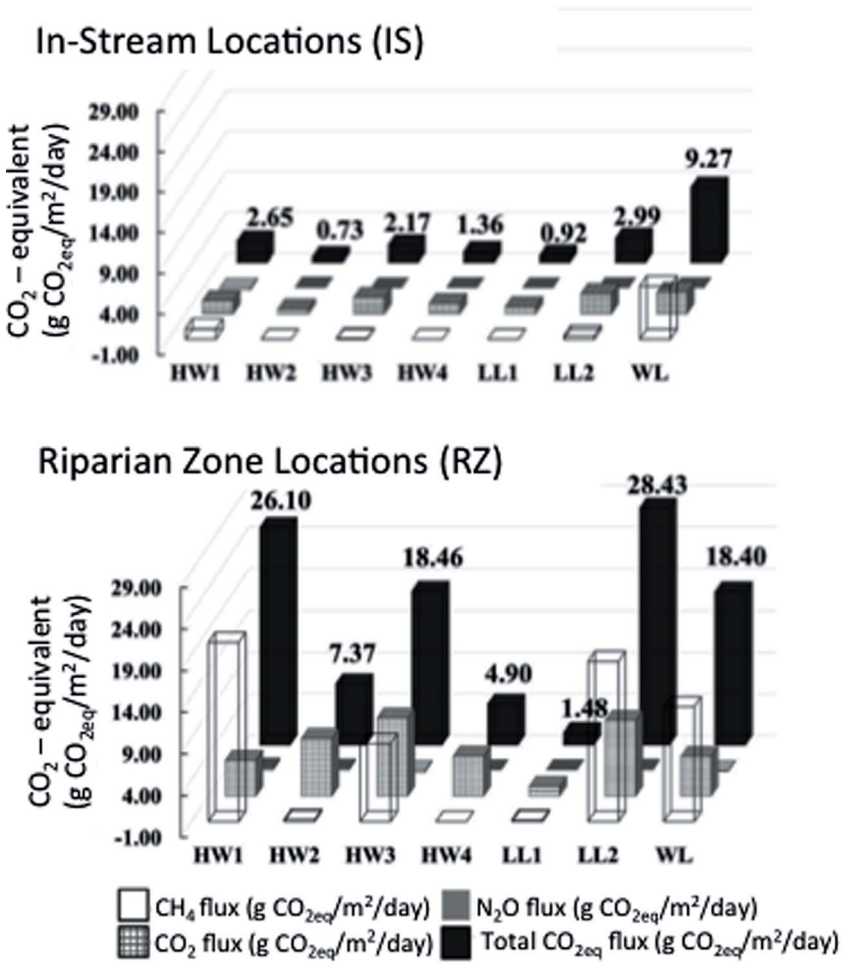

Fig. 4 Bar graphs illustrating total CO_2-equivalent (CO_{2eq}) emissions, and total CO_2, N_2O and CH_4 fluxes in CO_2-equivalent at riparian (RZ) and in-stream (IS) locations for stream reaches HW1–4, LL1–2, and WL over the study period (see Fig. 1 for acronym definitions).

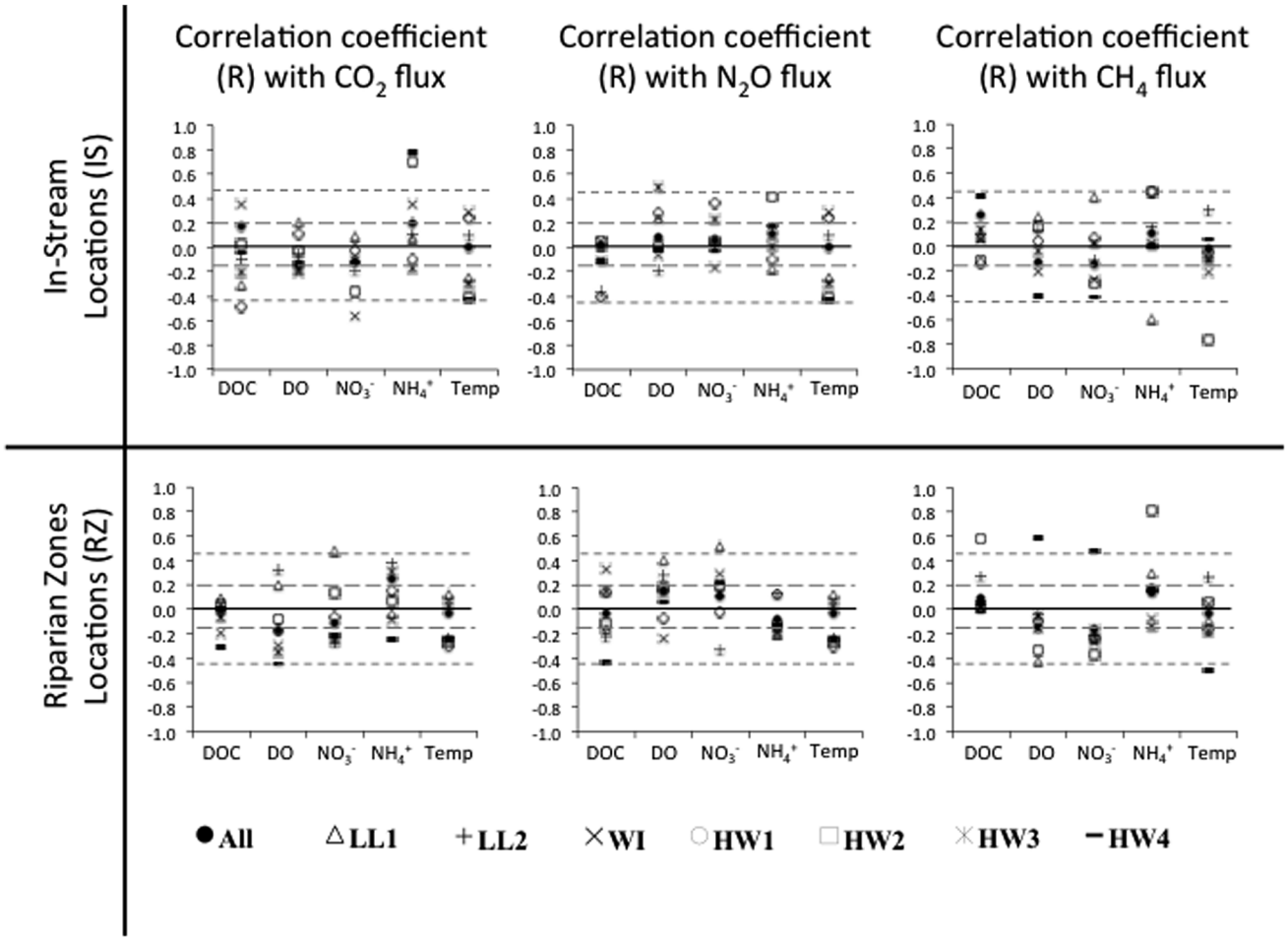

Fig. 5 Correlation coefficient between CO_2, N_2O and CH_4 fluxes and dissolved organic carbon (DOC), dissolved oxygen (DO), nitrate (NO_3^-), ammonium (NH_4^+), and groundwater temperature (Temp) for in-stream (upper) and riparian (lower) locations over the study period. *Acronyms*: All = all stream reaches combined ($n = 140$, if $r > 0.18$ then $p < 0.05$), HW1–4 = headwater locations 1 through 4, LL1 and LL2 = lowland locations 1 and 2, WL = wetland location ($n = 20$, if $r > 0.43$ then $p < 0.05$). Dashed lines at $r = \pm 0.18$ and $r = \pm 0.43$ indicate significant correlations ($p < 0.05$) for $n = 140$ and $n = 20$, respectively.

Discussion

Although fluxes varied significantly between locations (RZ *vs.* IS locations; headwater *vs.* lowland reaches…), reported fluxes were overall consistent with results published elsewhere. For instance, Riveros-Iregui and McGlynn (2009) reported daily CO_2 fluxes between 2.7 and 18.1 g C per m^2 per day in a northern Rocky Mountain watershed.[31] Elsewhere, Ambus and Christensen (1995) reported an average CH_4 flux value of 21.6 mg C per m^2 per day from temporarily flooded riparian areas,[32] while Merbach *et al.* (2002) reported CH_4 fluxes in the 0.09–90.5 mg C per m^2 per day range in riparian areas in Northern Germany.[33] With respect to N_2O, Jacinthe and Lal (2004) reported N_2O fluxes on the order of 0.32 mg N per m^2 per day in a forested system in Ohio,[2] while Fisher *et al.* (2014) reported N_2O fluxes from Indiana riparian zones in the 0.002–6.3 mg N per m^2 per day range.[6] Other studies also reported N_2O fluxes between −0.85 mg N per m^2 per day and 11.7 mg N per m^2 per day.[7,34]

As indicated in the Results section, when riparian fluxes (RZ) are compared to fluxes from in-stream locations (IS), total CO_{2eq} emissions are approximately 5 times higher at RZ locations than IS locations, with most CO_{2eq} driven by CH_4 production at wet sites (*i.e.* WL and LL2 sites, and mucky soil-influenced headwater HW1 and HW3 sites). This is consistent with wet/mucky sites being hot spots of greenhouse gas (GHG) emissions in the landscape, especially in terms of CH_4 emission due to low DO levels and high organic matter content.[3–5,35] However, these sites represent only a small surface area at the watershed scale (<10%, see Gomez *et al.* 2016)[35] or a small fraction of the entire stream length (see Fig. 1), suggesting that on a total areal basis at the stream or watershed scale, other non-wetland/mucky soil-influenced locations (*e.g.* LL1 or HW2 or HW4 type sites) may produce a larger amount of GHG.

In addition, on a gas-by-gas basis, no clear differences in N_2O fluxes between RZ and IS locations were observed, while CO_2 fluxes, and CH_4 at some locations were significantly larger at RZ locations than IS locations. Although both RZ and IS locations present aerobic conditions (DO > 2 mg L^{-1}), riparian zone soils likely contained higher soil organic carbon than in-stream locations, as suggested by the higher DOC concentration at RZ

locations than IS locations (Fig. 2). This is consistent with higher rates of aerobic respiration (CO_2 emission) at RZ locations than IS locations being associated with higher DOC concentrations at RZ locations than IS locations. The higher DOC in riparian zones than at in-stream locations is likely due to the fact that riparian zones are known to accumulate organic carbon due to their location in the landscape, especially near the outlet of the watershed (WL, LL2 and LL1) where wetland-like conditions dominate.[10] The higher DOC at RZ locations than IS locations is also consistent with terrestrial environment accumulating more organic matter than in-stream locations. Unlike CO_2, the differences in CH_4 fluxes between sites and locations were however mainly tied to the presence of hydromorphic soils like those found at the WL, LL2, and HW1 and HW3 sites, rather than just riparian *vs.* in-stream locations. As indicated earlier, this is consistent with wetland soils being hot spots of CH_4 production at the watershed scale due to enhanced methanogenesis stemming from widespread saturated conditions and organic rich soils.[3–5,14,15]

Beyond specific differences in GHG fluxes between RZ and IS locations, GHG fluxes were generally not consistently correlated to any of the potential drivers targeted in this study, namely DOC, DO, NO_3^-, NH_4^+, and groundwater temperature, suggesting that when all reaches are considered, these potential drivers do not seem to be good indicators of N_2O, CO_2, or CH_4 fluxes, at least during summer baseflow conditions and across the range of locations studied here (Fig. 5). However, it is important to note that this does not imply that these parameters do not affect GHG emissions. For instance, at the HW1 sites where mucky wet soils are present (Fig. 1), NH_4^+ is significantly ($p < 0.05$) positively correlated to CH_4 both at IS and RZ locations, which is consistent with the often observed accumulation of NH_4^+ in organic rich wet environment where methanogenesis occurs (produces CH_4) and where nitrification (strictly aerobic process) is limited by anoxia.[10,34] However, data illustrate than meaningful correlations do not consistently occur across all sites, and that when all the sites are considered together, DOC, DO, NO_3^-, NH_4^+, and groundwater temperature generally remain poorly correlated to GHG emissions in stream reaches across the watershed, except maybe for DOC and CH_4 at IS locations. This suggests that for the range of locations studied here, and for summer baseflow conditions, these water quality parameters offer little opportunity to predict GHG emission for generalization purposes. From a process standpoint, although soil or water biogeochemical conditions in the first 50 cm of the soil profile are generally considered to be good indicators of soil biogeochemical conditions near the soil surface,[8–10] it is possible that the lack of specific correlations between these biogeochemical condition indicators (DOC, DO, NO_3^-, NH_4^+, and groundwater temperature) and GHG fluxes is due to the fact that these are measured in piezometers (20–40 cm deep), even though the water table was within 15 cm of the ground surface at all locations. Nevertheless, it is likely that over longer periods of time, some of these variables (*e.g.* temperature) may become good predictors of GHG emission. Indeed, on an annual basis, other studies have shown that CO_2 and temperature are often significantly positively correlated and that temperature correlations with CO_2 flux can be useful in assessing possible behaviors of forest soils in response to changing temperature conditions.[36,37]

Nevertheless, for summer baseflow conditions, landscape position seems to be a better indicator of the magnitude of GHG fluxes across locations than water quality/water biogeochemistry indicators. Indeed, CO_2 fluxes are consistently several times higher at RZ locations than at IS exposed sediment locations, while CH_4 fluxes are consistently higher at sites with hydromorphic soil conditions (WL, LL2, HW1, HW3) than at sites with drier soils. Mapping of the entire stream length, and subsequently placing mapped stream reach sections in groups representing the various reaches studied here might therefore yield better results than regression/correlation analysis between water quality parameters and GHG fluxes to predict GHG fluxes at the floodplain scale over the entire length of the stream. Although we realize that measurements of a broader range of flow conditions across an entire year are needed to fully quantify the relative benefits of geomorphologically based approaches *vs.* regression/correlation approaches, Gomez *et al.* (2016) nevertheless demonstrated that landscape hydrogeomorphic characteristics were better predictors of GHG fluxes across a range of locations (wetland, lowland, riparian area, lower hillslopes, upper hillslope) than water quality indicators in this watershed over a two-year period.[35] Other studies have also linked soil respiration (CO_2 emission) to the structure and morphology of the landscape (*i.e.*, riparian zones *versus* hillslopes),[23,24] while others suggest clear differences in N_2O or CH_4 emissions between upland soils and wetlands.[8,15,22]

Ultimately, although more data need to be collected over multiple seasons and/or years to fully comprehend the relative importance of potential drivers of GHG fluxes at the reach scale across the whole watershed (*i.e.* landscape position *vs.* water quality indicators), this initial investigation allowed us to identify areas of the stream/floodplain most likely to generate significant greenhouse gas emissions to the atmosphere. As strategies are developed to further constrain GHG emission for whole watersheds over an annual basis, our data, along with other studies,[8,23,24] suggest that hydrogeomorphic approaches linking landscape characteristics (*e.g.* topography, soil type, soil moisture) to GHG fluxes at the soil–atmosphere interface are a promising avenue for research to generalize estimates of GHG fluxes along mountain stream reaches.

Acknowledgements

This project was supported by a US Geological Survey 104B grant (Award# 61103-10081) to P. Vidon through the New York Water Resources Institute in partnership with the New York Department of Environmental Conservation – Hudson River Estuary Program. Satish Serchan was supported though the US Department of Agriculture Forest Service Federal Pathway Program during his time at SUNY-ESF. The support of the New York State Energy Research and Development Authority (NYSERDA) in providing funds for the monitoring at the Arbutus Watershed and Huntington Forest is also greatly appreciated. The authors would also like to thank Pat McHale,

Joshua Gomez, Cheryl Glor, and the staff of the Adirondack Ecological Center in Newcomb, NY, for help in the field and laboratory.

References

1 IPCC, Climate Change 2013, *The Physical Science Basis. Contribution of Working Group I to the Fifth Assessment Report of the Intergovernmental Panel on Climate Change*, ed. T. F. Stocker, D. Qin, G.-K. Plattner, M. Tignor, S. K. Allen, J. Boschung, A. Nauels, Y. Xia, V. Bex and P. M. Midgley, Cambridge University Press, Cambridge, United Kingdom and New York, NY, USA, p. 1535, 2013, DOI: 10.1017/cbo9781107415324.

2 P. A. Jacinthe and R. Lal, Effects of soil cover and land-use on the relations flux-concentration of trace gases, *Soil Sci.*, 2004, **69**(4), 243–259.

3 S. Ullah and T. R. Moore, Biogeochemical controls on methane, nitrous oxide, and carbon dioxide fluxes from deciduous forest soils in eastern Canada, *J. Geophys. Res.: Biogeosci.*, 2011, **116**, G03010, DOI: 10.1029/2010jg001525.

4 M. R. Turetsky, A. Kotowska, J. Bubier, N. B. Dise, P. Crill, E. R. C. Hornibrook, K. Minkkinen, T. R. Moore, I. H. Myers-Smith, H. Nykänen, D. Olefeldt, J. Rinne, S. Saarnio, N. Shurpali, E. S. Tuittila, J. M. Waddington, J. R. White, K. P. Wickland and M. Wilmking, A synthesis of methane emissions from 71 northern, temperate, and subtropical wetlands, *Global Change Biol.*, 2014, **20**, 2183–2197.

5 J. L. Morse, M. Ardón and E. S. Bernhardt, Greenhouse gas fluxes in southeastern US coastal plain wetlands under contrasting land uses, *Ecol. Appl.*, 2012, **22**(1), 264–280.

6 K. Fisher, P. A. Jacinthe, P. Vidon, X. Liu and M. E. Baker, Nitrous oxide emission from cropland and adjacent riparian buffers in contrasting hydrogeomorphic settings, *J. Environ. Qual.*, 2014, **43**(1), 338–348, DOI: 10.2134/jeq2013.06.0223.

7 P. A. Jacinthe, J. S. Bills, L. P. Tedesco and R. C. Barr, Nitrous Oxide Emission from Riparian Buffers in Relation to Vegetation and Flood Frequency, *J. Environ. Qual.*, 2012, **41**, 95–105.

8 P. Vidon, J. A. Jacinthe, X. Liu, K. Fisher and M. Baker, Hydrobiogeochemical controls on riparian nutrient and greenhouse gas dynamics: 10 years post-restoration, *J. Am. Water Resour. Assoc.*, 2014, **50**(3), 639–652.

9 P. Groffman, K. Butterbach-Bahl, W. Fulweiler, A. Gold, J. Morse, E. Stander, C. Tague, C. Tonitto and P. Vidon, Incorporating Spatially and Temporally Explicit Phenomena (Hotspots and Hot Moments) in Denitrification Models, *Biogeochemistry*, 2009, **93**, 49–77, DOI: 10.1007/s10533-008-9277-5.

10 P. Vidon, C. Allan, D. Burns, T. P. Duval, N. Gurwick, S. Inamdar, R. Lowrance, J. Okay, D. Scott and S. Sebestyen, Hot spots and hot moments in riparian zones: Potential for improved water quality management, *J. Am. Water Resour. Assoc.*, 2010, **46**(2), 278–298.

11 J. J. Beaulieu, J. L. Tank, S. K. Hamilton, W. M. Wollheim, R. O. Hall Jr, P. J. Mulholland, B. J. Peterson, L. R. Ashkenas, L. W. Cooper, C. N. Dahm, W. K. Dodds, N. B. Grimm, S. L. Johnson, W. H. McDowell, G. C. Poole, H. M. Valett, C. P. Arango, M. J. Bernot, A. J. Burgin, C. L. Crenshaw, A. M. Helton, L. Johnson, J. M. O'Brien, J. D. Potter, R. W. Sheibley, D. J. Sobota and S. M. Thomas, Nitrous oxide emission from denitrification in stream and river networks, *Proc. Natl. Acad. Sci. U. S. A.*, 2011, **108**(1), 214–219, DOI: 10.1073/pnas.1011464108.

12 D. Butman and P. A. Raymond, Significant efflux of carbon dioxide from streams and rivers in the United States, *Nat. Geosci.*, 2011, **4**, 839–842.

13 S. F. Werner, B. A. Browne and C. T. Driscoll, Three-dimensional spatial patterns of trace gas concentrations in baseflow-dominated agricultural streams: implications for surface–ground water interactions and biogeochemistry, *Biogeochemistry*, 2012, **107**, 319–338, DOI: 10.1007/s10533-010-9555-x.

14 L. O. Hedin, J. C. von Fischer, N. E. Ostrom, K. P. Kennedy, M. G. Brown and G. P. Robertson, Thermodynamic constraints on nitrogen transformations and other biogeochemical processes at soil–stream interfaces, *Ecology*, 1998, **79**(2), 684–703.

15 R. J. Naiman, H. Decamps and M. E. McClain, *Riparia: Ecology, Conservation, and Management of Streamside Communities*, Academic Press, 2010.

16 T. Kasahara and A. R. Hill, Effects of riffle-step restoration on hyporheic zone chemistry in N-rich lowland streams, *Can. J. Fish. Aquat. Sci.*, 2005, **63**, 120–133.

17 P. A. Jacinthe, P. M. Groffman, A. J. Gold and A. Mosier, Patchiness in Microbial Nitrogen Transformations in Ground-Water in a Riparian Forest, *J. Environ. Qual.*, 1998, **27**, 156–164.

18 J. C. Clement, G. Pinay and P. Marmonier, Seasonal dynamics of denitrification along topohydrosequences in three different riparian wetlands, *J. Environ. Qual.*, 2002, **31**, 1025–1037.

19 P. Vidon and A. R. Hill, Denitrification and Patterns of Electron Donors and Acceptors in Eight Riparian Zones with Contrasting Hydrogeology, *Biogeochemistry*, 2004, **71**, 259–283, DOI: 10.1007/s10533-004-9684-1.

20 R. J. Naiman and J. M. Melillo, Nitrogen budget of a subarctic stream altered by beaver (*Castor canadensis*), *Oecologia*, 1984, **62**(2), 150–155.

21 C. A. Johnston and R. J. Naiman, Boundary dynamics at the aquatic–terrestrial interface: the influence of beaver and geomorphology, *Landsc. Ecol.*, 1987, **1**(1), 47–57.

22 M. S. Castro, P. A. Steudler, J. M. Melillo, J. D. Aber and R. D. Bowden, Factors controlling atmospheric methane consumption by temperate forest soils, *Global Biogeochem. Cycles*, 1995, **9**(1), 1–10.

23 D. A. Riveros-Iregui, R. E. Emanuel, D. J. Muth, B. L. McGlynn, H. E. Epstein, D. L. Welsch, V. J. Pacific and J. M. Wraith, Diurnal hysteresis between soil CO_2 and soil temperature is controlled by soil water content, *Geophys. Res. Lett.*, 2007, **34**, L17404, DOI: 10.1029/2007gl030938.

24 V. J. Pacific, B. L. McGlynn, D. A. Riveros-Iregui, D. L. Welsch and H. E. Epstein, Landscape structure, groundwater dynamics, and soil water content influence soil respiration across riparian–hillslope transitions in the Tenderfoot Creek Experimental Forest, Montana, *Hydrol. Process.*, 2010, **25**(5), 811–827.

25 M. J. Mitchell, D. J. Raynal and C. T. Driscoll, *Response of Adirondack Ecosystems to Atmospheric Pollutants and Climate Change at the Huntington Forest and Arbutus Watershed: Research Findings and Implications for Public Policy. Synthesis Report. New York State Energy Research and Development Authority (NYSERDA)*, Albany, New York, 2009.

26 S. F. Christopher, B. D. Page, J. L. Campbell and M. J. Mitchell, Contrasting stream water NO_3^- and Ca_2^+ in two nearly adjacent catchments: the role of soil Ca and forest vegetation, *Global Change Biol.*, 2006, **12**(2), 364–381.

27 R. C. Somers, *Soil Classification, Genesis, Morphology and Variability of Soils Found within the Central Adirondack Region of New York*, State University of New York, College of Environmental Science and Forestry, Syracuse, 1986.

28 M. R. McHale, J. J. McDonnell, M. J. Mitchell and C. P. Cirmo, A field-based study of soil water and groundwater nitrate release in an Adirondack forested watershed, *Water Resour. Res.*, 2002, **38**(4), 2–16.

29 L. S. Clesceri, A. E. Greenberg and A. D. Eaton, *Standard Methods for the Examination of Water and Waste Water*, American Public Health Association, Washington, DC, 1998.

30 P. A. Jacinthe and W. A. Dick, Soil Management and Nitrous Oxide Emissions from Cultivated Fields in Southern Ohio, *Soil Tillage Res.*, 1997, **41**, 221–235.

31 D. A. Riveros-Iregui and B. L. McGlynn, Landscape structure control on soil CO_2 efflux variability in complex terrain: Scaling from point observations to watershed scale fluxes, *J. Geophys. Res.: Biogeosci.*, 2009, **114**(G2), G02010.

32 P. Ambus and S. Christensen, Spatial and seasonal nitrous oxide and methane fluxes in Danish forest-, grassland-, and agroecosystems, *J. Environ. Qual.*, 1995, **24**(5), 993–1001.

33 W. Merbach, T. Kalettka, C. Rudat and J. Augustin, Trace gas emissions from riparian areas of small eutrophic inland waters in Northeast-Germany, in *Wetlands in Central Europe*, Springer Berlin Heidelberg, 2002, pp. 235–244.

34 M. M. Hefting, R. Bobbink and H. de Caluwe, Nitrous oxide emission and denitrification in chronically nitrate-loaded riparian buffer zones, *J. Environ. Qual.*, 2003, **32**, 1194–1203.

35 J. Gomez, P. Vidon, J. Gross, C. Beier, J. Caputo and M. Mitchell, Estimating greenhouse gas emission at the soil–atmosphere interface on forested watersheds of the US Northeast, *Environ. Monit. Assess.*, 2016, **188**(5), 1–16, DOI: 10.1007/s10661-016-5297-0.

36 E. A. Davidson, E. Belk and R. D. Boone, Soil water content and temperature as independent or confounded factors controlling soil respiration in a temperate mixed hardwood forest, *Global Change Biol.*, 1998, **4**(2), 217–227.

37 S. Kang, S. Doh, D. Lee, V. Jin and J. S. Kimball, Topographic and climatic controls on soil respiration in six temperate mixed-hardwood forest slopes, Korea, *Global Change Biol.*, 2003, **9**(10), 1427–1437.